

Design of Composites Based on Lithium Titanate and Carbon Nanomaterials for High-Power Lithium-Ion Batteries [†]

Irina Stenina ^{1,*} , Andrey Desyatov ² and Tatiana Kulova ³

¹ Kurnakov Institute of General and Inorganic Chemistry of the Russian Academy of Sciences, 31, Leninsky Prospekt, 119991 Moscow, Russia

² Department of Industrial Ecology, D. Mendeleev University of Chemical Technology of Russia, 9, Miusskaya pl., 125047 Moscow, Russia; avdesyatov@mail.ru

³ Frumkin Institute of Physical Chemistry and Electrochemistry of the Russian Academy of Sciences, 31-4, Leninsky Prospekt, 119071 Moscow, Russia; tkulova@mail.ru

* Correspondence: stenina@igic.ras.ru; Tel.: +7-495-775-6585

[†] Presented at the 1st International Electronic Conference on Processes: Processes System Innovation, 17–31 May 2022; Available online: <https://ecp2022.sciforum.net>.

Abstract: The composite nanomaterials based on hydrothermally or sol-gel synthesized $\text{Li}_4\text{Ti}_5\text{O}_{12}$ and both nitrogen-doped and undoped carbons were prepared and investigated by XRD, SEM, low-temperature nitrogen adsorption, dc-measurements, charge-discharge tests, cyclic voltammetry, and electrochemical impedance spectroscopy. Carbon nanotube introduction provides the formation of a highly conductive 3D network resulting in increase in electronic conductivity, lithium diffusion, and thus improvement of rate-capability and cycling stability of the composites.

Keywords: lithium-ion battery; $\text{Li}_4\text{Ti}_5\text{O}_{12}$; CNT; composite; anode



Citation: Stenina, I.; Desyatov, A.; Kulova, T. Design of Composites Based on Lithium Titanate and Carbon Nanomaterials for High-Power Lithium-Ion Batteries. *Eng. Proc.* **2022**, *19*, 3. <https://doi.org/10.3390/ECP2022-12663>

Academic Editor:
Andrey Yaroslavtsev

Published: 30 May 2022

Publisher's Note: MDPI stays neutral with regard to jurisdictional claims in published maps and institutional affiliations.



Copyright: © 2022 by the authors. Licensee MDPI, Basel, Switzerland. This article is an open access article distributed under the terms and conditions of the Creative Commons Attribution (CC BY) license (<https://creativecommons.org/licenses/by/4.0/>).

1. Introduction

Lithium-ion batteries are widely used in electronic devices, first of all, owing to their high energy density, low self-discharge, and relatively small weight. $\text{Li}_4\text{Ti}_5\text{O}_{12}$ is considered as a promising anode material for lithium-ion batteries, primarily due to low degradation during cycling and high safety. However, its electronic and ionic conductivities are relatively low that limits its practical application. The design of composites with conductive materials (e.g., with carbon), is one of the approaches to improve the electrochemical properties of materials. In this work, the $\text{Li}_4\text{Ti}_5\text{O}_{12}$ /carbon nanomaterial composites were prepared by ball-milling. Different synthesis methods (sol-gel and hydrothermal) of lithium titanate as well as both nitrogen-doped and undoped carbons were used to compare their effect on specific electrochemical capacity and rate capability of the obtained composites.

2. Materials and Methods

Lithium titanate was prepared by a sol-gel method (LTO_{sg}) in the presence of citric acid (final calcination temperature 800 °C) or hydrothermally (LTO_{H} , final calcination temperature 400 °C), using procedures described elsewhere [1,2]. To prepare the LTO/C composites a mixture of lithium titanate and 5 or 10 wt% carbon nanomaterial was ball-milled at 200 rpm for 1 h and 5 min for LTO_{sg} and LTO_{H} , respectively. Carbon nanotubes (CNTs), agglomerates of graphene particles (carbon nanoflakes, CNFs), N-doped ones (N-CNTs and N-CNFs, respectively) or CNTs (CNFs) together with 5 wt% carbon black (CB) were used as carbon nanomaterials. Hereinafter, the obtained composites are denoted as $\text{LTO}_{\text{H}}/5\text{CNT}$, $\text{LTO}_{\text{H}}/10\text{N-CNF}$, $\text{LTO}_{\text{sg}}/5\text{CB}/5\text{N-CNT}$, etc. indicating the carbon nanomaterial used and its amount.

X-ray diffraction (Rigaku D/MAX 2200 diffractometer with $\text{CuK}\alpha$ radiation) was used to examine the crystal structure. Their morphology and particle size were studied

by scanning electron microscopy using a Carl Zeiss NVision 40. The specific surface area of the samples was measured by BET (Brunauer-Emmett-Teller) method at $-196\text{ }^{\circ}\text{C}$ on a Sorbtometr-M instrument.

Electrochemical characteristics were studied using hermetically sealed three-electrode electrochemical cells with lithium as counter and reference electrodes. The working electrodes were prepared by pasting a mixture of the composite (85 wt%), carbon black (10 wt%), and polyvinylidene fluoride binder (5 wt%) dissolved in N-methyl-2-pyrrolidone on a stainless-steel grid (to be used as a current collector). The amount of the active material on the electrode was $10\text{--}15\text{ mg/cm}^2$. The electrodes were pressed at 0.1 GPa and dried at $120\text{ }^{\circ}\text{C}$ under vacuum. The Celgard 2300 polypropylene membrane and 1 M LiPF_6 solution in a 1:1:1 mixture of ethylene carbonate, diethyl carbonate, and dimethyl carbonate were used as the separator and the electrolyte, respectively. The cells (lithium metal | electrolyte | active material) were assembled in an argon-filled glove box and cycled using a ZRU 50 mA–10 V charge–discharge system (JSC NTTs Buster) at potentials in the range of 1–3 V and at current densities in the range of 20–6400 mA/g. Cyclic voltammograms were recorded using an Elins P-8NANO electrochemical workstation at different scanning rates (0.1–1.6 mV/s). Electrochemical impedance spectra were obtained using an Elins Z500 PRO analyzer in the frequency range of 10 Hz to 2 MHz at an amplitude of 80 mV.

3. Results and Discussion

3.1. Material Characterization

According to PDF-2 database file no. 72-0426, all of the diffraction peaks in the X-ray diffraction patterns of the composites based on LTO_H and LTO_sg can be assigned to the cubic $\text{Li}_4\text{Ti}_5\text{O}_{12}$ (Figure 1). In the case of the LTO_H /carbon composites, a weak reflection at $2\theta \approx 24\text{--}26^{\circ}$ results from the (002) crystallographic plane of graphene [3]. In the case of the composites based on LTO_sg , no reflections of graphene and carbon nanotubes were detected. Apparently, this is due to the low content of carbon materials in the composites and/or the low intensity of their reflexes against the reflection (111) of LTO_sg .

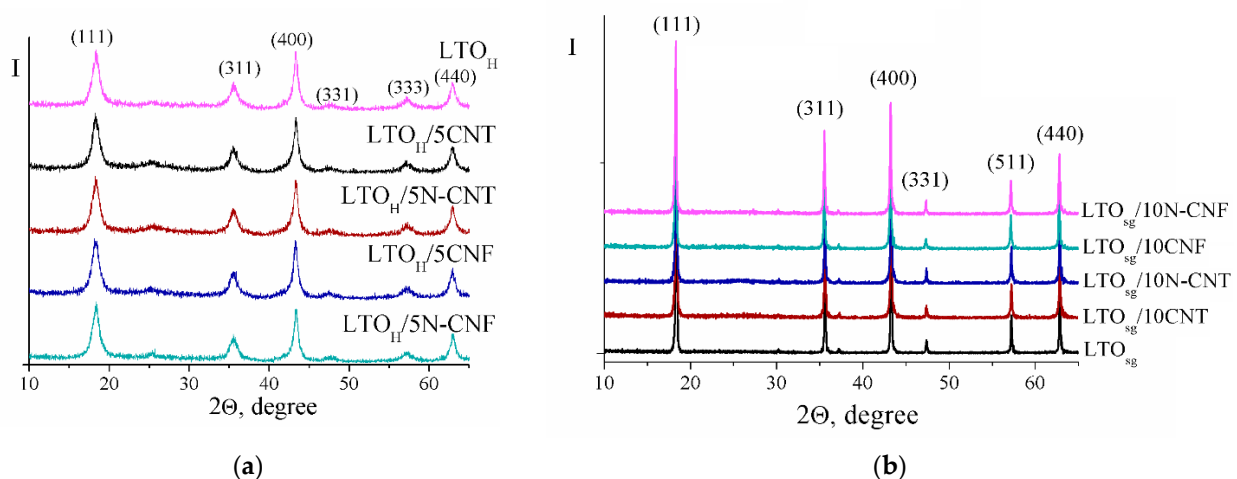


Figure 1. X-ray diffraction patterns of the composites based on LTO_H (a) and LTO_sg (b).

Figure 2 illustrates the SEM images of the composites based on lithium titanate prepared hydrothermally and by sol-gel method. In the composites based on LTO_H and carbon nanotubes, the latters are homogeneously distributed over the LTO_H surface, indicating the formation of a well-connected conductive network on the lithium titanate particles (Figure 2b). Unlike the composites based on LTO_H , carbon nanotubes are unevenly distributed over the surface of lithium titanate prepared by sol-gel method, forming agglomerates of several microns in size (Figure 2e). The dark-grey areas in the backscattered

electron SEM images of the LTO/CNFs composites (Figure 2c,f) indicate large agglomerates of graphene among lithium titanate particles (light-grey areas) suggesting no effective contact between them.

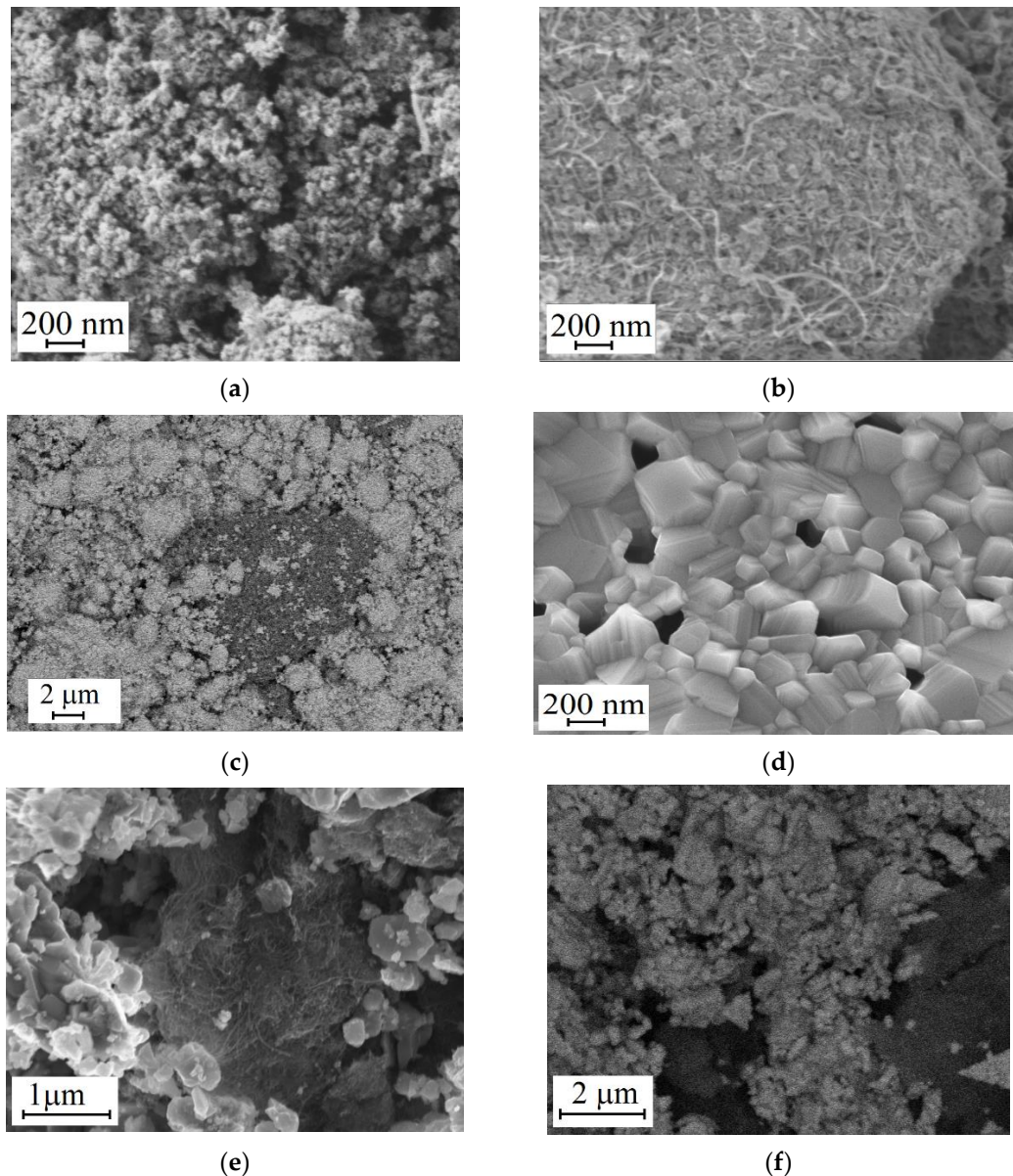


Figure 2. SEM images of LTO_H (a), LTO_H/CNT (b), LTO_H/CNF (c), LTO_{sg} (a), LTO_{sg}/CNT (b), and LTO_{sg}/CNF (c) in the secondary (a,b,d,e) and backscattered electron modes (c,f).

The BET surface area is 598, 287, 1198, and 1028 m²/g for CNTs, N-CNTs, CNFs, and N-CNFs, respectively. Undoped CNTs and CNFs have larger BET surface areas than that of nitrogen-doped carbon nanomaterials. The specific surface area of LTO_H and LTO_{sg} are 103 and 5–7 m²/g, respectively. Among the obtained composites, the composites with CNTs have the highest BET surface area.

Ball-milling of lithium titanate with CNTs or CNFs leads to a pronounced increase in the dc conductivity of the obtained composites. The dc conductivity of the composites based on LTO prepared hydrothermally increases in the series LTO_H << LTO_H/N-CNF < LTO_H/CNF < LTO_H/CNT < LTO_H/N-CNT. Electron conductivity of the LTO_H/CNT composite is 7 times lower than that of the LTO_H/nitrogen-doped CNT composite (1.33 S/cm). In the case of the composites with carbon nanoflakes, electron conductivity is much lower,

due to a non-effective contact between CNFs and lithium titanate particles (9.6×10^{-5} and 6.7×10^{-5} S/cm for the composites with CNFs and nitrogen-doped CNFs, respectively). The dc conductivity of the composites based on LTO_{sg} increases from 0.01 to 0.36 S/cm in the series $\text{LTO}_{\text{sg}}/\text{10N-CNF} < \text{LTO}_{\text{sg}}/\text{10CNF} < \text{LTO}_{\text{sg}}/\text{10CNT} \approx \text{LTO}_{\text{sg}}/\text{5CB}/\text{5N-CNT} < \text{LTO}_{\text{sg}}/\text{10N-CNT}$.

The Nyquist plots for the LTO_{H} -based composites consist of a semicircle (correspond to the charge transfer process at the electrode/electrolyte interface) and a straight line, which represents lithium-ion diffusion (the Warburg impedance) in the high- and low-frequency regions, respectively. The Li^+ diffusion coefficients of LTO_{H} , $\text{LTO}_{\text{H}}/\text{5CNT}$, and $\text{LTO}_{\text{H}}/\text{5CNF}$ calculated using the Warburg impedance are 1.1×10^{-13} , 1.2×10^{-12} , and 8.0×10^{-14} cm^2/s , respectively.

3.2. Electrochemical Performance

Figure 3a,b show cycling performance of the composites based on $\text{Li}_4\text{Ti}_5\text{O}_{12}$ prepared hydrothermally and by sol-gel method, respectively. At a low current density (20 mA/g), the discharge capacities of all of the composites are in the range of 140–170 mAh/g. Taking into account the low electrochemical capacity of the carbon nanomaterials in the potential range of 1–3 V and their content in the composites, the discharge capacity of the $\text{LTO}_{\text{H}}/\text{CNT}$, $\text{LTO}_{\text{sg}}/\text{10CNF}$ and $\text{LTO}_{\text{sg}}/\text{5CB}/\text{5N-CNT}$ composites approaches the theoretical value of $\text{Li}_4\text{Ti}_5\text{O}_{12}$ (175 mAh/g). At high current densities, the best rate capability was found for the composites with CNTs.

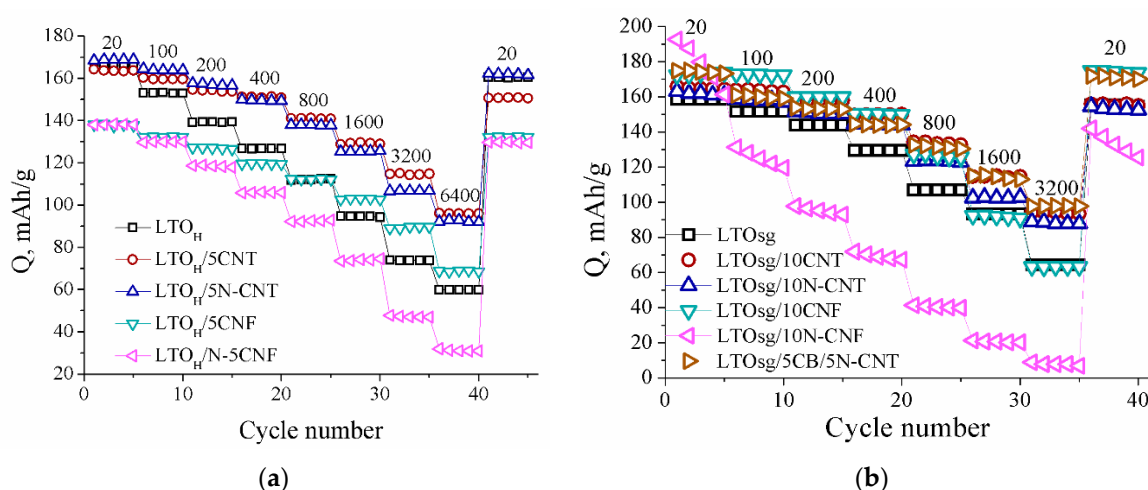


Figure 3. Cycling performance of the composites based on LTO_{H} (a) and LTO_{sg} (b). The current densities (mA/g) are shown in the Figure.

4. Conclusions

The composites based on $\text{Li}_4\text{Ti}_5\text{O}_{12}$ synthesized by hydrothermal and sol-gel methods and carbon nanomaterials were prepared by a simple ball-milling method. The introduction of latters leads to an increase in the electrical conductivity of the composites and the reversible discharge capacity even at high charge/discharge rates. In the composites with carbon nanotubes, as latters can bridge $\text{Li}_4\text{Ti}_5\text{O}_{12}$ particles a high-conductive network forms providing fast electron and lithium transport. In the case of lithium titanate prepared by sol-gel method, the highest discharge capacity (97 mAh/g at ~18C rate) is observed for composites with CNTs and carbon black. In the case of $\text{Li}_4\text{Ti}_5\text{O}_{12}$ prepared hydrothermally, at ~18C rate, the discharge capacities of lithium titanate with CNTs and N-doped CNTs are 107 and 114 mAh/g, respectively. The use of carbon nanoflakes is less efficient since their large agglomerates are retained in the composite even after ball-milling and, hence, the composite is less uniform and there is no a network of highly conductive contacts between the lithium titanate particles.

Author Contributions: Conceptualization, I.S.; methodology, I.S., A.D. and T.K.; investigation, T.K., A.D. and I.S.; data curation, I.S.; writing—original draft preparation, T.K. and I.S.; writing—review and editing, I.S.; supervision, I.S. and T.K.; project administration, I.S.; funding acquisition, I.S. All authors have read and agreed to the published version of the manuscript.

Funding: This research was funded by the Russian Foundation for Basic Research, grant No. 20-08-00769.

Institutional Review Board Statement: Not applicable.

Informed Consent Statement: Not applicable.

Data Availability Statement: The data presented in this study are available on request from the corresponding author.

Acknowledgments: This research was performed using the equipment of the JRC PMR IGIC RAS.

Conflicts of Interest: The authors declare no conflict of interest.

References

1. Stenina, I.A.; Kulova, T.L.; Skundin, A.M.; Yaroslavtsev, A.B. High grain boundary density $\text{Li}_4\text{Ti}_5\text{O}_{12}$ /anatase- TiO_2 nanocomposites as anode material for Li-ion batteries. *Mater. Res. Bull.* **2016**, *75*, 178–184. [[CrossRef](#)]
2. Stenina, I.A.; Kulova, T.L.; Skundin, A.M.; Yaroslavtsev, A.B. Effects of carbon coating from sucrose and PVDF on electrochemical performance of $\text{Li}_4\text{Ti}_5\text{O}_{12}$ /C composites in different potential ranges. *J. Solid State Electrochem.* **2018**, *22*, 2631–2639. [[CrossRef](#)]
3. Nethravathi, C.; Rajamathi, M. Chemically modified graphene sheets produced by the solvothermal reduction of colloidal dispersions of graphite oxide. *Carbon* **2008**, *46*, 1994–1998. [[CrossRef](#)]